

# Miniaturized and Bandwidth Improvement of Bandpass Filter using A Quarter Wavelength Resonator

Dwi Astuti Cahyasiwi<sup>1\*</sup>, Amsaluddin Zanetti<sup>1</sup>, Dian Widi Astuti<sup>2</sup>, Galih Adhi Yoga<sup>3</sup>

<sup>1</sup>*Department of Electrical Engineering, University of Muhammadiyah Prof. Dr. HAMKA, East Jakarta, 13830, Indonesia*

<sup>2</sup>*Department of Electrical Engineering, Universitas Mercu Buana, West Jakarta, Indonesia*

<sup>3</sup>*Research Center for Telecommunication, National Research and Innovation Agency (BRIN), Bandung, West Java, Indonesia*

\*Corresponding author. Email: dwi.cahyasiwi@uhamka.ac.id

**Abstract—** The miniaturization of radio frequency (RF) and microwave filters is crucial in modern communication systems, particularly in space-constrained environments such as portable, wearable, or integrated multi-band platforms. In this study, a compact single band-pass filter (BPF) is proposed using an L-shaped resonator loaded with a via-through hole. The incorporation of the via allows the creation of a quarter-wavelength resonator, which significantly reduces the physical size to 44.6% compared to traditional half-wavelength resonators commonly used in band-pass filters. Additionally, the via contributes to an improved impedance bandwidth. Two L-shaped resonators are arranged in a back-to-back configuration to realize a second-order filter response. The structure is excited through a stub-loaded transmission line that couples the signal from port one to port two. To validate the proposed design, the filter was fabricated and measured. Experimental results demonstrate a -3 dB fractional bandwidth (FBW) exceeding 25% at the centre frequency of 3.2 GHz, with a measured insertion loss of -1.662 dB across the passband, indicating good performance for compact filter applications.

**Keywords—** A-Quarter Wavelength Resonator; Filter; Miniaturized; Second-Order; Via Through-Hole.

## I. INTRODUCTION

Bandpass filters (BPFs) play a critical role in modern communication systems, enabling the selective transmission of signals within a desired frequency range while suppressing unwanted frequencies. As wireless technologies advance toward higher integration, lower power consumption, and compact form factors, particularly in applications such as 5G, IoT devices, wearable electronics, and satellite communications; the demand for miniaturized and high-performance BPFs has grown significantly. A miniaturized bandpass filter offers a compact solution without compromising essential electrical characteristics such as insertion loss, bandwidth, return loss, and out-of-band rejection. The miniaturization of filters is essential for space-constricted environments, specifically in systems that integrate multiple filters or require multi-band operations. Techniques such as substrates integrated waveguides [1] - [6], folded structure [7] - [9], defected ground structures (DGS) [10] - [14], tree dimension resonators [15] - [17] and metamaterials [18] - [20] have been widely explored to reduce the physical size of filters while maintaining desired performance.

A triple-band band-pass filter reduces the size of its resonators using a folding of a half wavelength resonator technique; however, the overall filter size remains relatively large, and the bandwidth -3 dB also below 10% which is relatively narrow [7]. Substrate integrated wave guide added with double complementary split ring resonator (CSRR) is design to obtain a bandpass filter with wide stop band, though

it claimed a miniaturized design the overall dimension is still bulky [1].

Metamaterial in the form of a complementary split-ring resonator (CSRR) is incorporated to realize a wideband bandpass filter with multiple transmission zeros [12] whereas in [3], a dual-band bandpass filter is investigated using a meandered slot surrounded by a substrate integrated waveguide for miniaturization purposes. A bandpass filter using three step-impedance resonators (SIRs) [10] was claimed to operate in the ultra-wideband (UWB) frequency range; however, it exhibited three band notches that interrupted continuous operation across the UWB spectrum. All previous designs employ half-wavelength resonators; however, the simplest approach to miniaturization is to shorten the resonators to quarter-wavelength by adding a via through-hole at the end of the resonators.

In [9] dual bandpass filter using the combination of tree quarter and half wavelength resonators was studied and reduced the dimension to 38%. Using third order filter the design still need more space to accommodate all the three resonators. This study integrates bandwidth enhancement and miniaturization in the design of a BPF by employing folded quarter-wavelength resonators arranged in a back-to-back configuration. The reverse orientation of the resonators modifies the electric and magnetic field distributions within the structure, which is expected to reduce the external quality factor of the filter, thereby increasing the bandwidth. The design improves upon the folded half-wavelength resonator presented in [7] by achieving a wider bandwidth and a more compact structure of 44.6 % through the addition of a via through-hole at the end of

the resonator arm. The proposed filter operates at 3.3 GHz with a  $-3$  dB bandwidth scalable for 5G and satellite applications.

## II. METHOD

The illustrated structure in Figure 1 shows the detailed physical dimensions of a planar bandpass filter comprising two quarter-wavelength resonators placed in a back-to-back configuration. The resonators are implemented using microstrip lines and terminated with via through holes to ground at their open ends, labeled with white circles. The parameters  $L_0, L_f, L_1, L_2, W_0, W_f, W_1, W_2, S_1, S_2$  and  $R_0$  define the lengths, widths, spacings, and corner radius of the resonator arms, all the dimension can be seen in Table I. The spacing  $S_1$  influences the coupling between the feed lines and the resonators, while  $S_2$  governs the inter-resonator coupling. The via holes at the ends of the resonator arms provide a short-circuit termination, enabling miniaturization and improving the filter performance.

The proposed filter consists of two quarter-wavelength resonators ( $R_1$  and  $R_2$ ) arranged in a back-to-back configuration, as depicted in Figure 2(a) where the input coupled-line is directly connected to the  $50 \Omega$  port 1 ( $P_{IN}$ ), and the other end of the resonator is connected to the  $50 \Omega$  port 2 output ( $P_{OUT}$ ). The layout in Figure 2(b) illustrates the coupling topology, where  $M_{x1}$  and  $M_{y2}$  represent the input and output coupling to the resonators,  $M_{12}$  denotes the inter-resonator coupling, and  $M_{11}$  and  $M_{22}$  indicate the self-coupling terms. This configuration facilitates enhanced bandwidth and compactness compared to conventional half-wavelength designs.

In designing the size of the resonator, the length of the resonator will affect the resonant frequency of the resonator that will be produced. To obtain a frequency ( $f$ ), the length of the resonator is made with a length of  $\frac{1}{2} \lambda_g$  or a length of  $\frac{1}{4} \lambda_g$ . The value of  $\lambda$  is obtained using the general equation for transmission lines. In microstrip transmission lines, the value of  $\lambda$  is also influenced by the size of the effective dielectric constant of the material used. In designing this filter, the resonant frequency of the resonator is targeted to match the center frequency ( $f_c$ ) specified for the desired filter. The length of one wave in a microstrip can be calculated using (1).

$$\lambda_g = \frac{\lambda_0}{f(\text{GHz})\sqrt{\epsilon_r, \text{eff}}} \quad (1)$$

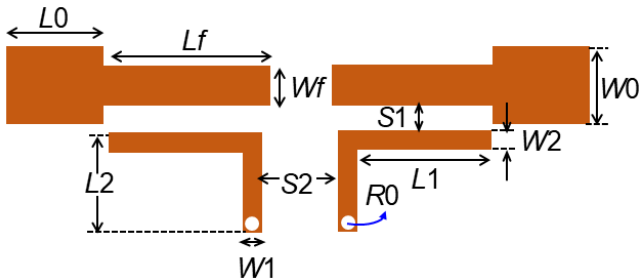


Figure 1 Geometric design of the proposed single-bandpass filter

TABLE I. PARAMETER DIMENSION OF THE PROPOSED DESIGN ALL UNIT DIMENSION IN MM

$W_0$	$W_f$	$W_1$	$W_2$	$L_0$
4.86	2.86	1	1	7
$L_f$	$L_1$	$L_2$	$S_1 = S_2$	$R_0$
12.5	11.5	6.5	0.5	0.3

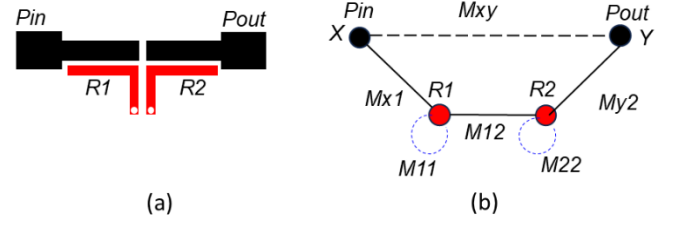


Figure 2 (a) The filter structure and (b) the coupling mechanism

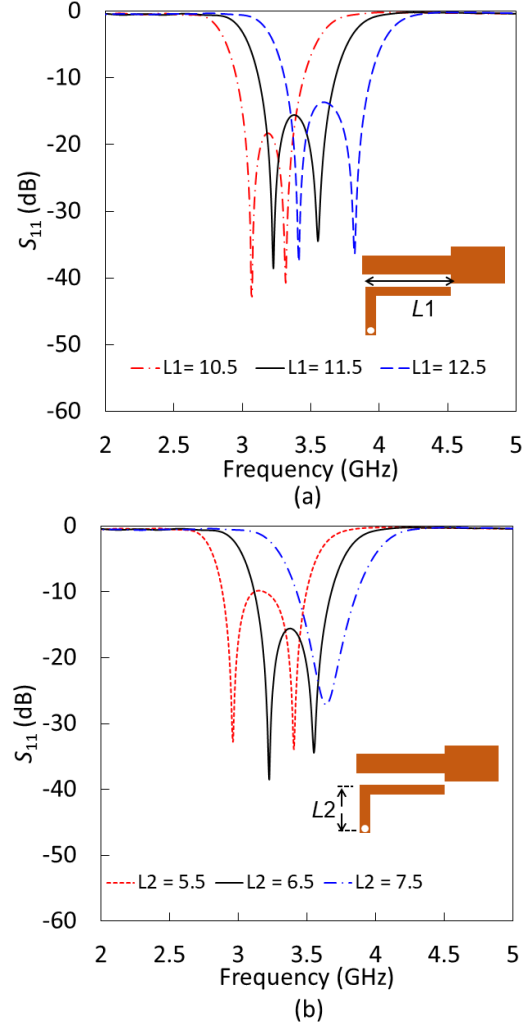


Figure 3 (a)  $S_{11}$  response with  $L_2 = 6.5$  and  $L_1$  varied (b)  $S_{11}$  response with  $L_1 = 11.5$  and  $L_2$  varied (all unit in mm)

## III. RESULTS AND DISCUSSION

The resonator lengths  $L_1$  and  $L_2$  strongly govern the resonant characteristics of the proposed BPF structure. As shown in Figure 3(a), with  $L_2$  fixed at 6.5 mm increasing  $L_1$  from 10.5 to 12.5 mm varied from 10.5 mm to 12.5 mm, the resonant frequencies shift toward higher values results in an upward shift of the resonant frequencies while preserving the overall  $-10$  dB impedance bandwidth. The response consistently exhibits two distinct minima, indicative of second-order filter behavior. In contrast, Figure 3(b) demonstrates that with  $L_1$  fixed at 11.5 mm and varied from 5.5 to 7.5 mm, both the impedance bandwidth and resonant frequency are altered. Notably, when  $L_2$  is set to 7.5 mm, the resonant frequency is 3.7 GHz, but the  $-10$  dB impedance bandwidth becomes narrower and exhibits a single minimum, indicating that the filter no longer behaves as a second-order design.

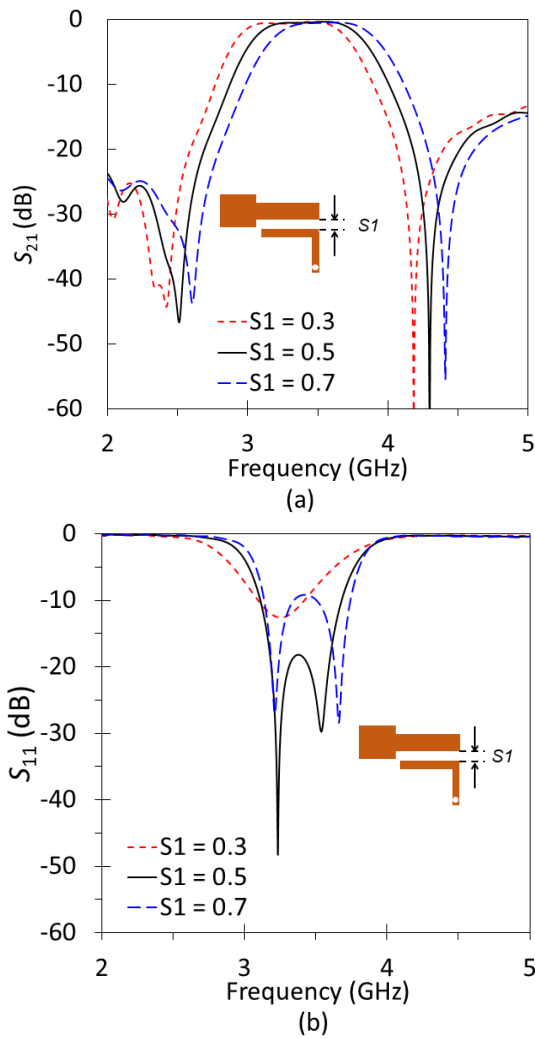


Figure 4 The response of (a)  $S_{21}$  and (b)  $S_{11}$  with  $S1$  variation (all unit in mm)

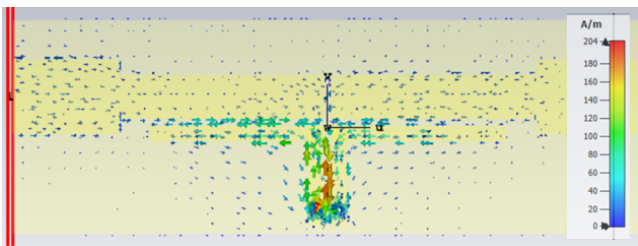


Figure 5 The surface current of the proposed design at 3.58 GHz

The structure in Figure 4 is used to investigate the  $S_{21}$ , and  $S_{11}$  values with different gap  $S1$ . Figure 4(a) shows that the increased  $S1$  from 0.3 to 0.7 mm leads to a degradation in selectivity as observed in the  $S_{21}$  response. Figure 4(b) shows that the increased of  $S1$  weakens the electromagnetic coupling between the resonator sections, resulting in reduced energy transfer and a narrower -10 dB bandwidth impedance. This behavior occurs because a wider gap decreases the mutual capacitance, thereby lowering the coupling coefficient.

Figure 5 illustrates the current distribution at the operating frequency of 3.3 GHz. The current flows from port one through the transmission line, continues to the stub, and is then coupled into the L-shaped resonator. The coupling begins at the horizontal arm connected to the stub and extends toward the arm containing the via hole. The stub on the input side also couples to the stub on the output transmission line, which subsequently excites the second L-shaped resonator. The opposing placement of the two L-shaped resonators enables

magnetic coupling between them. The BPF optimization was performed using CST Studio Suite software, resulting in a simulated single-band response with a -10 dB bandwidth impedance of 565 MHz ranges from 3.11 – 3.68 GHz, or 17.1%.

The simulated insertion loss ( $S_{21}$ ) was -0.51 dB, with a -3 dB bandwidth passband of 781 MHz (3.04 – 3.82 GHz) or 22.8% FBW at 3.42 GHz centre frequency. The prototype was fabricated using Roger Duroid 5880 with permittivity of 2.2 and thickness of 1.575 mm as shown in Figure 6(a) and the measurement set-up is shown in Figure 6(b), (c). The  $S_{11}$  measurement of BPF results shown in Figure 7(a) where the centre frequency shifted to the lower side and the value of  $S_{11}$  increased compare to the simulation results, however, the -10 dB bandwidth impedance was improved to 645 MHz (2.91 – 3.56 GHz) or 20.1%. The measurement results of  $S_{21}$  in Figure 7(b) also depicted a wider -3 dB bandwidth of 825 MHz (2.88 – 3.71 GHz), or 25.7% centred at 3.2 GHz frequency.

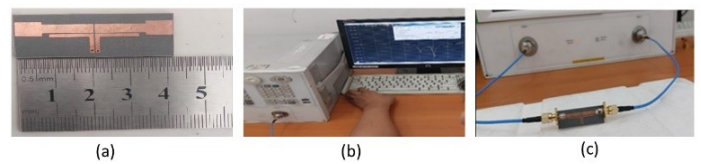


Figure 6 (a) The fabricated design, (b)  $S_{11}$  measurement capture and (c) measurement set-up of BPF

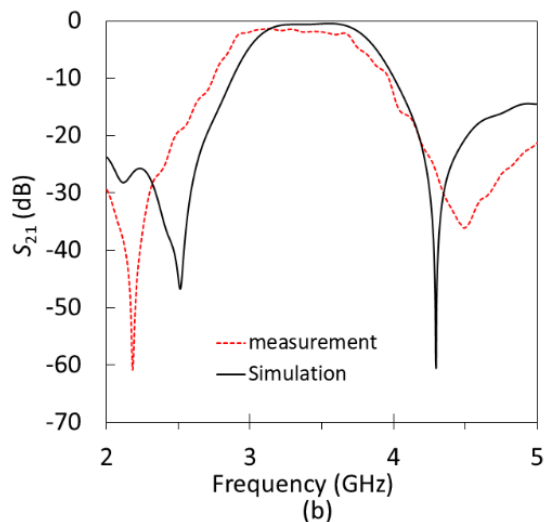
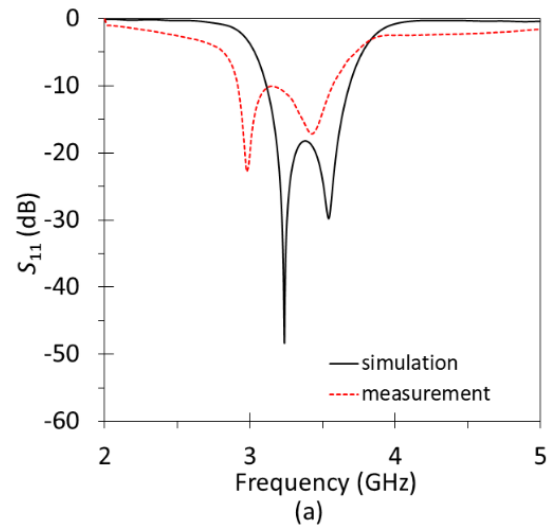
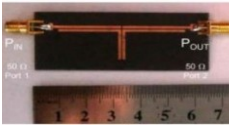



Figure 7 Simulation and measurement results of the proposed BPF (a)  $S_{11}$  and (b)  $S_{21}$

TABLE II. PARAMETER DIMENSION OF THE PROPOSED DESIGN ALL UNIT DIMENSION IN MM

Parameter	Reference [7]	This work
Dimension (mm)	 P = 65 L = 20	 P = 41.5 L = 14
Dimension ( $\lambda g^{3*}$ )	0.048×0.715×0.22	0.048×0.456×0.15
Frequency (GHz) (Sim./Meas.)	3.25 / 3.27	<b>3.3 / 3.25</b>
FBW (-3 dB) (%) (Sim./Meas.)	8.09 / 9.14	<b>22.80 / 25.70</b>
Insertion Loss (dB) (Sim./Meas.)	-0.35 / -0.8	<b>0.54 / 1.66</b>
$S_{11}$ (dB) (Sim./Meas.)	-17.0 / -19.6	<b>-20.86 / -11.08</b>

\* $\lambda g$  is the free space wavelength at the center frequency

TABLE III. THE COMPARISON OF THE PREVIOUS WORK AND THE PROPOSED DESIGN

Ref	Dimension ( $\lambda g^2$ )	Frequency (GHz)/FBW (%)	Insertion loss	$S_{11}$ (dB)
[1]	0.227	10.10/23.88	0.8	-15
[6]	0.085	8.88/17.57	1.29	-19
[7]	0.034	3.25/9.14	0.8	-10
[10]	0.066	6.85/114	2	-15
[21]	0.078	2.5/12	1	-25
<b>This work</b>	<b>0.021</b>	<b>3.2/25.7</b>	<b>1.66</b>	<b>-11.08</b>

\* $\lambda g$  is the free space wavelength at the center frequency

Though the bandwidth -3 dB increased, the *insertion loss* (IL) degraded to -1.622 dB. The discrepancy between the simulation and measurement attributed to discontinuities at connector launches, solder pads, or feedline transitions. The insertion loss and return loss remain within acceptable levels, ensuring good signal integrity. Therefore, the wide bandwidth enhances system performance without significantly compromising filter selectivity.

The comparison of BPF using L resonator with and without a via through hole from the previous study [7] is shown in Table II. In terms of physical dimensions, the proposed design achieves a more compact dimension compared to the previous study resulting a size reduction of 44.6%. The proposed design exhibits a significantly wider fractional bandwidth (FBW) of 25.70% compared to 9.14% in [7]. While the insertion loss is slightly higher at -1.66 dB than -0.8 dB in [7], the  $S_{11}$  reaches -20.86 dB in simulation but degrades to -11.08 dB in measurement, compared to -19.6 dB in [7]. The proposed design offers a more compact footprint and a substantially broader bandwidth, though with slightly higher insertion loss and lower measured return loss. As shown in Table III compared with other compact bandpass filters, it achieves the most compact profile. Although [10] demonstrates the widest FBW among the referenced studies, it also exhibits the highest insertion loss. Hence, the proposed design is well-suited for applications requiring a low-profile filter with a wide FBW.

#### IV. CONCLUSION

In conclusion, a single-band band-pass filter operating at 3.2 GHz was successfully designed and fabricated, achieving significant miniaturization and bandwidth enhancement using

a via-through-hole resonator. The fabricated results showed excellent performance with an insertion loss of -1.66 dB, and a -3 dB bandwidth of 25.7%. The overall filter dimensions were reduced by approximately 44.6%, while the bandwidth improved by 257% compared to conventional half-wavelength resonators, confirming the effectiveness of the proposed design.

#### ACKNOWLEDGEMENT

The authors would like to thank Research Center for Telecommunication, National Research and Innovation Agency for providing CST software.

#### REFERENCES

- [1] U. Senathipathi and S. Krishnan, "Compact substrate integrated waveguide bandpass filter with wide stopband tunable transmission zeros," *Electromagnetics*, 2025, doi: 10.1080/02726343.2025.2492266.
- [2] D. W. Astuti, Y. Wahyu, F. Y. Zulkifli, and E. T. Rahardjo, "Hybrid HMSIW Cavity Antenna with a Half Pentagon Ring Slot for Bandwidth Enhancement," 2020.
- [3] H. Al-Darraj and H. Al-Saedi, "Compact Dual-Band BPF Based on Loaded SIW with Meandered Slot Line for 5G and Beyond Applications," *Progress In Electromagnetics Research M*, vol. 128, pp. 89–98, 2024, doi: 10.2528/PIERM24070803.
- [4] Q. Liu, H. Qian, D. W. Zhang, K. Gong, and Q. K. Liu, "Compact Highly-Selective Bandpass Filter Based on Triple-Mode Ridge Substrate Integrated Waveguide Cavity," *IEEE Microwave and Wireless Technology Letters*, vol. 33, no. 9, pp. 1274–1277, Sep. 2023, doi: 10.1109/LMWT.2023.3276794.
- [5] A. Iqbal, J. J. Tiang, S. K. Wong, S. W. Wong, and N. K. Mallat, "QMSIW-Based single and triple band bandpass filters," *IEEE Transactions on Circuits and Systems II: Express Briefs*, vol. 68, no. 7, pp. 2443–2447, Jul. 2021, doi: 10.1109/TCSII.2021.3055904.
- [6] G. Lin, Y. Dong, and X. Luo, "Miniaturized Quarter-Mode SIW Filters Loaded by Dual-Mode Microstrip Resonator With High Selectivity and Flexible Response," *IEEE Microwave and Wireless Components Letters*, vol. 32, no. 6, pp. 660–663, Jun. 2022, doi: 10.1109/LMWC.2022.3161619.
- [7] T. Firmansyah, M. Alaydrus, Y. Wahyu, E. T. Rahardjo, and G. Wibisono, "A highly independent multiband bandpass filter using a multi-coupled line stub-sir with folding structure," *IEEE Access*, vol. 8, pp. 83009–83026, 2020, doi: 10.1109/ACCESS.2020.2989370.
- [8] Q. Xue and J. Y. Jin, "Bandpass Filters Designed by Transmission Zero," vol. 65, no. 11, pp. 4103–4110, 2017.
- [9] J. Khalil and M. K. Saleem, "Design and Miniaturization of Dual Band Filter based on Quarter Wavelength Resonators," in *2023 International Conference on Energy, Power, Environment, Control, and Computing, ICEPECC 2023 - Proceedings*, Institute of Electrical and Electronics Engineers Inc., 2023, doi: 10.1109/ICEPECC57281.2023.10209496.
- [10] L. Wang, S. Yang, Q. Guo, B. Li, and L. Zhang, "Super compact and ultra-wideband bandpass filter with three band notches using triple-mode stepped impedance resonator and defected ground structure," *J Electromagn Waves Appl*, vol. 38, no. 10, pp. 1158–1175, 2024, doi: 10.1080/09205071.2024.2360552.
- [11] C. Li, Z. H. Ma, J. X. Chen, M. N. Wang, and J. M. Huang, "Design of a Compact Ultra-Wideband Microstrip Bandpass Filter," *Electronics (Switzerland)*, vol. 12, no. 7, Apr. 2023, doi: 10.3390/electronics12071728.
- [12] A. N. Ghazali and J. Hussain, "Broadband Bandpass Filter for UWB Networks with Multiple In-Band Transmission Zeros," *IETE J Res*, vol. 69, no. 8, pp. 5566–5573, 2023, doi: 10.1080/03772063.2021.1973588.
- [13] L. Su, J. Munoz-Enano, P. Velez, J. Martel, F. Medina, and F. Martin, "On the Modeling of Microstrip Lines Loaded with Dumbbell Defect-Ground-Structure (DB-DGS) and Folded DB-DGS Resonators," *IEEE Access*, vol. 9, pp. 150878–150888, 2021, doi: 10.1109/ACCESS.2021.3125775.
- [14] A. G. Neto, J. N. De Carvalho, J. C. E. Silva, C. G. M. Lima, R. A. Raimundo, and D. A. MacEdo, "Miniaturization of DGS Filter Based on Matryoshka Geometry Using Calcium Cobaltite Ceramic," in *20th SBMO/IEEE MTT-S International Microwave and Optoelectronics Conference, IMOC 2023*, Institute of Electrical and Electronics Engineers Inc., 2023, pp. 61–63, doi: 10.1109/IMOC57131.2023.10379697.
- [15] F. Liu, X. Liu, Z. Ma, L. A. Bian, P. Wen, and K. Da Xu, "Miniaturized Dual-Band Bandpass Filter Using Triple-Mode Dielectric Waveguide Resonators With Adjustable Capacity in Transmission Zeros," *IEEE Microwave and Wireless Technology Letters*, vol. 35, no. 6, pp. 670–673, 2025, doi: 10.1109/LMWT.2025.3550814.

- [16] Q. Yang *et al.*, "Compact Millimeter-Wave Wideband Bandpass Filter Design Using Triple-Mode Rectangular Ridge Resonator," *IEEE Microwave and Wireless Technology Letters*, vol. 34, no. 7, pp. 883–886, 2024, doi: 10.1109/LMWT.2024.3405074.
- [17] J. J. Yan, F. C. Chen, and R. C. Lin, "A Triple-Band Bandpass Filter Based on Triple-Mode Metal Block Resonators," *IEEE Microwave and Wireless Technology Letters*, vol. 35, no. 2, pp. 173–176, 2025, doi: 10.1109/LMWT.2024.3509141.
- [18] B. Pradhan and B. Gupta, "A Miniaturized Band-Reject Filter Using Metamaterial Structures on Silicon Substrate for X-Band Application," *IETE J Res*, vol. 67, no. 3, pp. 294–300, 2021, doi: 10.1080/03772063.2018.1540948.
- [19] A. Zermane, B. Sauviac, L. Djouablia, and A. Benghalia, "Tunability of metamaterial compact band-stop filters using YIG substrate," *J Electromagn Waves Appl*, vol. 33, no. 13, pp. 1726–1734, Sep. 2019, doi: 10.1080/09205071.2019.1632748.
- [20] B. Pradhan and B. Gupta, "A Miniaturized Band-Reject Filter Using Metamaterial Structures on Silicon Substrate for X-Band Application," *IETE J Res*, vol. 67, no. 3, pp. 294–300, 2021, doi: 10.1080/03772063.2018.1540948.
- [21] R. Zaker, S. Mojtaba, and S. Najjar Hosseini, "Miniaturized Bandpass Filter Design Utilizing Substrate-Integrated Metasurface in Coupled Dipole-Antenna Array with Harmonic Suppression," *IEEE Trans Antennas Propag*, 2025, doi: 10.1109/TAP.2025.3567835.